Atmospheric Teleconnection Patterns and Severity of Winters in the Laurentian Great Lakes Basin

Sergei Rodionov and Raymond Assel*
U.S. Department of Commerce
National Oceanic and Atmospheric Administration
Great Lakes Environmental Research Laboratory
Ann Arbor, Michigan 48105, U.S.A.

[Original manuscript received 10 May 2000; in revised form 3 August 2000]

ABSTRACT *We analyzed the relationship between an index of Great Lakes winter severity (winters 1950–1998) and atmospheric circulation characteristics. Classification and Regression Tree analysis methods allowed us to develop a simple characterization of warm, normal and cold winters in terms of teleconnection indices and their combinations. Results are presented in the form of decision trees. The single most important classifier for warm winters was the Polar/Eurasian index (POL). A majority of warm winters (12 out of 15) occurred when this index was substantially positive (POL > 0.23). There were no cold winters when this condition was in place. Warm winters are associated with a positive phase of the Western Pacific pattern and El Niño events in the equatorial Pacific. The association between cold winters and La Niña events was much weaker. Thus, the effect of the El Niño/Southern Oscillation (ENSO) on severity of winters in the Great Lakes basin is not symmetric. The structure of the relationship between the index of winter severity and teleconnection indices is more complex for cold winters than for warm winters. It takes two or more indices to successfully classify cold winters. In general, warm winters are characterized by a predominantly zonal type of atmospheric circulation over the Northern Hemisphere (type W1). Within this type of circulation it is possible to distinguish two sub-types, W2 and W3. Sub-type W2 is characterized by a high-pressure cell over North America, which is accompanied by enhanced cyclonic activity over the eastern North Pacific. Due to a broad southerly "anomalous" flow, surface air temperatures (SATs) are above normal almost everywhere over the continent. During the W3 sub-type, the polar jet stream over North America, instead of forming a typical ridge-trough pattern, is almost entirely zonal, thus effectively blocking an advection of cold Arctic air to the south. Cold winters tend to occur when the atmospheric circulation is more meridional (type C1). As with warm winters, there are two sub-types of circulation, C2 and C3. In the case of C2, the jet stream loops southward over the western part of North America, but its northern excursion over the eastern part is suppressed. In this situation, the probability of a cold winter is higher for Lake Superior than for the lower Great Lakes. Sub-type C3 is characterized by an amplifi-*

*Corresponding author's e-mail: Assel@glerl.noaa.gov

cation of the climatological ridge over the Rockies and the trough over the East Coast. The strongest negative SAT anomalies are located south of the Great Lakes basin, so that the probability of a cold winter is higher for the lower Great Lakes than for Lake Superior.

RÉSUMÉ *Nous analysons la relation entre un indice de la rigueur du froid hivernal des Grands Lacs (hivers 1950 à 1998) et les caractéristiques de la circulation atmosphérique. Les méthodes d'analyses selon un arbre de classification et de régression nous a permis de développer une caractérisation simple des hivers chauds, normaux et froids en termes d'indices de téléconnexions et de leurs combinaisons. Les résultats sont présentés sous la forme d'arbres de décisions. L'élément unique le plus important de classification des hivers chauds a été l'indice polaire/eurasien (POL). Les hivers chauds, en majorité (12 sur 15), ont eu lieu lorsque cet indice a été fortement positif (POL > 0,23). Il n'y a pas eu d'hivers froids lorsque cette condition a été en place. Les hivers chauds sont associés avec une phase positive de la configuration du Pacifique Ouest et du phénomène El Niño dans la région équatoriale du Pacifique. L'association entre les hivers froids et le phénomène La Niña a été beaucoup plus faible. Ainsi, l'effet de l'oscillation méridionale El Niño (ENSO) sur la rigueur des hivers dans le bassin des Grands Lacs n'est pas symétrique. La structure de la relation entre l'indice de la rigueur du froid hivernal et les indices de téléconnexions est plus complexe pour les hivers froids que pour les hivers chauds. On choisit deux ou plus d'indices pour classifier avec succès les hivers froids. En général, les hivers chauds sont caractérisés par la prédominance d'une circulation atmosphérique de type zonal sur l'hémisphère Nord (type W1). Avec ce type de circulation, il est possible de distinguer deux sous-types, W2 et W3. Le sous-type W2 est caractérisé par une cellule de haute pression sur l'Amérique du Nord et celle-ci est accompagnée par la mise en valeur d'une activité cyclonique sur l'est du Pacifique Nord. En raison d'une circulation méridionale anormale, les températures de l'air en surface sont au-dessus de la normale presque partout sur le continent. En présence d'un sous-type W3, le courant-jet polaire sur l'Amérique du Nord, au lieu de former une configuration typique crête/creux, est presque entièrement zonal, bloquant ainsi toute advection d'air froid arctique vers le sud . Les hivers froids tendent à se produire lorsque la circulation atmosphérique est plus méridionale (type C1). Tandis qu'avec des hivers chauds, il y a deux sous-types de circulation, C2 et C3. Dans le cas de C2, le courant-jet dévie vers le sud sur la partie ouest de l'Amérique du Nord., mais son excursion septentrionale sur la partie orientale est supprimée. Dans cette situation, la probabilité d'un hiver froid est plus grande pour le lac Supérieur que pour les Grands lacs inférieurs. Le sous-type C3 est caractérisé par une amplification de la crête climatologique sur les Rocheuses et du creux sur la Côte Est. Comme les anomalies négatives des températures de l'air en surface les plus fortes sont localisées au sud du bassin des Grands Lacs, la probabilité d'un hiver froid est plus grande pour les Grands lacs inférieurs que pour le lac Supérieur.*

1 Introduction

The Great Lakes constitute one of the world's largest freshwater resources and play a vital role in the regional and national economies of the United States and Canada. About 24.7 million Americans and 8.5 million Canadians live in the Great Lakes basin[1]. The severity of the weather each winter in the Great Lakes region has a sig-

[1]Great Lakes Commission and Environment Canada, http://www.great-lakes.net/refdesk/almanac/glpeople.html

nificant impact on the economy of both nations. This is exemplified by two extreme winters that occurred in the 1990s. During the cold 1994 winter, air temperatures were much below average, lake effect snowfall was enhanced, costs for fuel usage for space heating were greater than average, road maintenance costs were greater than average, property damage due to ice and snow storms was extensive, and costs for Coast Guard assistance to ships were greater than average because ice cover was above average (Assel et al., 1996). This contrasts sharply with the mild 1998 winter. During the winter of 1998 air temperatures in the Great Lakes region were at or near record highs, which dramatically reduced utility costs associated with space heating. Also, because lake-ice cover during that winter was at a record low, the costs associated with Coast Guard maintenance of navigation routes and assistance to ships were the lowest in over a decade (Assel et al., 2000).

Atmospheric circulation is the major factor causing changes in the winter severity from one year to another. A distinctive feature of the interannual variability of the large-scale atmospheric circulation is the substantial degree of its spatial organization in the form of teleconnection patterns (Wallace and Gutzler, 1981). These patterns, or preferred modes, of atmospheric circulation are characterized by in-phase or out-of-phase variations of sea-level pressure (SLP) or geopotential heights in specific areas known as "centres of action." Teleconnections are most prominent during the winter season and may weaken or disappear during the warm time of the year (Wallace et al., 1993). Barnston and Livezey (1987) also showed that many of the strong winter patterns have statistically significant persistence in the middle of their active period, a result consistent with the previous work of Namias (1978, 1986). Teleconnections are an effective, parametric way to describe atmospheric circulation. They have proven to be a valuable tool to understand better the complex relationships between the planetary-scale circulation and regional climatic variations (Yarnal and Leathers, 1988; Leathers et al., 1991; Assel and Rodionov, 1998; Serreze et al., 1998).

A major mode of atmospheric variability over the Northern Hemisphere is the Pacific/North American (PNA) pattern (Wallace and Gutzler, 1981). The PNA pattern is a broadband feature of the atmospheric low-frequency variability, which remains the same on both the interannual and intermonthly timescales (Esbensen, 1984). The importance of the PNA for the North American climate results from the fact that this pattern represents a departure from the mean upper-level flow over the continent, which features a climatological ridge in the west and a trough in the east. The PNA index measures an amplification or damping of this stationary wave (Leathers and Palecki, 1992). The index was found to be strongly correlated with monthly temperatures in many U.S. climatic divisions, with the centres of highest correlation in the Pacific Northwest and the Southeast (Leathers et al., 1991).

One of the most striking features of the PNA pattern is its teleconnection with the El Niño/Southern Oscillation (ENSO) events in the tropical Pacific (Horel and Wallace, 1981; Mo et al., 1998). During warm events the PNA index has a tendency to be positive, but during cold events it tends to be negative (Yarnal and Diaz 1986). It

was somewhat surprising to us, when in our previous work (Assel and Rodionov, 1998) we found that annual maximum ice cover on the Great Lakes had a relatively poor association with the PNA index and, at the same time, a substantial ENSO signal. Assel (1998) found that during the six strongest warm ENSO events since 1950 (based on the value of a Multivariate ENSO Index (Wolter and Timlin, 1998) prior to the 1997 ENSO) the mean of modelled annual maximum ice cover was 15% lower than the mean over the rest of the winters between 1950 and 1994, a difference statistically significantly at the 95% level. This inconsistency in the relationship between the severity of winters in the Great Lakes basin, the PNA and ENSO events was one of the motivations for the present work.

It is relevant to note that ENSO is not the only source responsible for exciting the PNA pattern. Some observational and modelling studies indicate that the atmospheric response to the extratropical sea surface temperature (SST) anomalies may be even stronger than the response to the tropical SST anomalies (Lau and Nath, 1990; Wallace and Jiang, 1992; Wallace et al., 1990, 1992). On the other hand, the PNA is not the sole pattern that occurs during ENSO events. The Western Pacific (WP) and the Tropical/Northern Hemisphere (TNH) patterns were also found to be related to ENSO (Horel and Wallace, 1981; Barnston and Livezey, 1987; Mo et al., 1998). These two patterns can make a substantial difference in the response of winter temperatures in the Great Lakes basin to ENSO events and the PNA.

Assel and Rodionov (1998) have demonstrated that a positive (negative) phase of the TNH pattern facilitates above (below) normal ice cover on the Great Lakes. The North American centres of action of the TNH are shifted eastward with respect to those of a PNA pattern so as to be out of phase with it. One of those centres, which is located north of the Great Lakes, coincides with the area of strongest correlation between ice cover and 700-hPa height over the Northern Hemisphere.

Another teleconnection pattern that significantly affects the climate of eastern North America is the North Atlantic Oscillation (NAO). Its effect is stronger for the most eastward located lake, Lake Ontario, than for the other Great Lakes (Assel and Rodionov, 1998). Kushnir and Wallace (1989) identify the NAO and the PNA as the two dominant modes of variability in the interannual timescale. Unlike the PNA, WP and TNH patterns, variations in the NAO appear to be relatively more independent from ENSO (Rogers, 1984).

When examining relationships between the severity of winters in the Great Lakes basin and large-scale atmospheric circulation, it is important to consider not only separate teleconnection patterns, but their combinations as well. As Yarnal and Leathers (1988) noted, the interaction between spatially distinct teleconnections may be responsible for a significant portion of previously unexplained variance in surface climate variables. This has been confirmed in both regional and hemispheric studies. Thus, Bunkers et al. (1996) found it important to consider a combination of the PNA and TNH patterns to characterize temperature variation in the Northern Plains. The positive phase of the PNA and the negative phase of TNH manifest themselves in warmer winter temperature in this region, and negative phases of both

lead to below-normal temperatures. Yarnal and Leathers (1988) suggested that a combined action of the PNA and NAO might be important to the climate of the United States. They computed a multiple linear regression of these indices with Pennsylvania winter temperature, which showed that 50% of the variance is explained by the linear combination of these two variables.

Several studies have examined a combined effect of the NAO and ENSO events. According to Rogers (1984), the NAO and Southern Oscillation (SO) together are associated with significant pressure and height variations over most of the Northern Hemisphere except for Siberia and portions of western North America. Both the NAO and SO significantly influence geopotential height and SLP distributions over the western Atlantic and eastern North America. Mysak et al. (1996) showed that during three simultaneous NAO and ENSO events of 1972/73, 1982/83 and 1991/92, there were larger-than-normal sea-ice extents in Hudson Bay and in the Baffin Bay-Labrador Sea region. During these three events, cold surface air temperature (SAT) anomalies produced by atmospheric circulation changes lasted for several seasons and appeared to be an important contributing mechanism for the ice anomalies. Barnston and He (1996) examined a combined effect of the NAO and ENSO on SAT anomalies over all of North America. They constructed NAO composite maps partitioned by the Southern Oscillation Index (SOI) that showed both agreeing and conflicting influences of these two indices. It is evident from these maps that the western portions of North America tend to be affected more by the SOI than the NAO, and vice versa for the eastern portions. The central latitudes are affected by both phenomena, whose influences may either oppose or enhance one another.

The objective of this study is to improve our understanding of what teleconnection indices or interaction between indices drive the interannual variations in winter conditions in the Great Lakes basin and to describe the atmospheric circulation patterns associated with warm, normal and cold categories of winters. The paper is organized as follows. Section 2 describes the Winter Severity Index (WSI) and the dataset of teleconnection indices. Based on the WSI, all winters are broken into three categories: warm, normal and cold. Section 3 outlines the method used in this study to determine those teleconnection indices and their combinations that are most characteristic of each of these categories. The method presents the relationship between the WSI and teleconnection indices in the form of decision (or classification) trees, or alternatively, as IF-THEN rules. These decision trees and the corresponding rules are analyzed in Section 4 to determine which terminal node of the trees can be considered as a separate type of atmospheric circulation. Section 5 describes those individual teleconnection patterns that play an important role in the construction of the trees. Section 6 discusses the types of atmospheric circulation associated with warm, normal and cold winters in the Great Lakes basin. Each type is described using the composite maps of 700-hPa height and SAT anomalies. The difference in the position of the jet stream over North America between these types of circulation is also demonstrated. The results are summarized in Section 7.

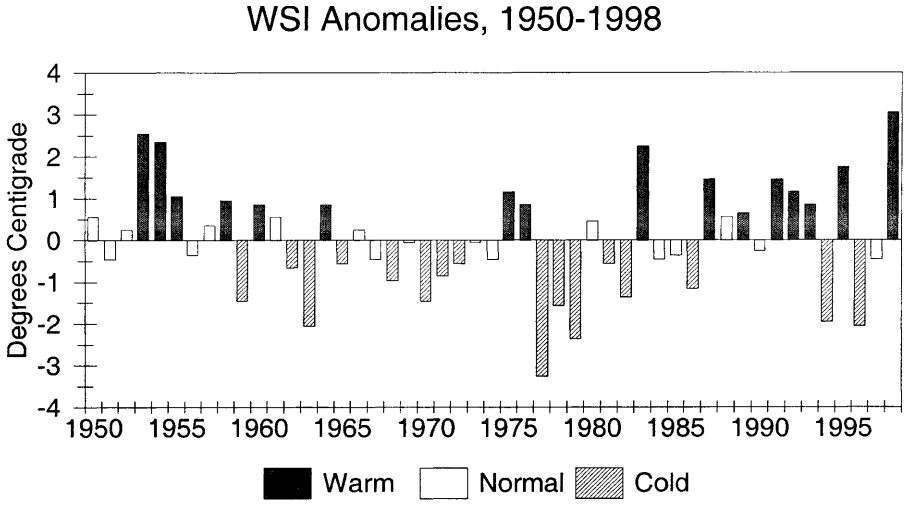

Fig. 1 WSI anomalies, presented as deviations from the average value for the 1950–1998 period, and their classification into warm, normal and cold winters.

2 Data

a *Winter Severity Index*

A regional WSI was developed by Snider (in Quinn et al., 1978) as a measure of the temperature severity of the winter over the Great Lakes from late fall to late winter. It is defined as the 4-month average (November to February) of the monthly average temperatures at Duluth, MN, Sault Ste. Marie, MI, Detroit, MI, and Buffalo, NY. Snider used the index to place the thermal severity of the 1977 winter in the historical context of the past 200 years. He found that winter 1977 was the 5th coldest since 1777. Other studies also use the WSI to place anomalous Great Lakes winters in historical perspective (Assel et al., 1985, 1996, 2000). The WSI is highly correlated with the annual maximum ice cover extent over the Great Lakes (Assel et al., 1985) and it is also used to model the annual maximum ice cover and in climate studies to simulate decadal trends in annual maximum ice cover over the past century (Magnuson et al., 1997). The WSI was also used in the analysis of regional Great Lakes response to warm El Niño events (Assel, 1998).

In this study we used the WSI for the period 1950–1998 to match it with the data available on the teleconnection indices. The range of variations of the WSI was broken into three categories with approximately an equal number of cases in each category. This was achieved by using two arbitrary breakpoints of –0.50°C and +0.5°C. The winters with WSI anomalies less than –0.5°C are referred to as cold, the winters with WSI anomalies greater than +0.5°C are referred to as warm, and the winters between these two categories are referred as normal. The WSI and assignment of categories are presented in Fig. 1.

b *Teleconnection Indices*

In addition to the PNA, NAO, WP, TNH and ENSO indices described in the introduction, we used three other teleconnection indices that have received less attention in the scientific literature, but potentially may influence the North American winter climate: Polar/Eurasian (POL), East Pacific (EP) and East Atlantic (EA). All these indices are routinely calculated by the Climate Prediction Center (CPC) and are available through the Internet[2]. The diagnostic procedure used by the CPC to identify teleconnection patterns is the Rotated Principal Component Analysis – RPCA (Barnston and Livezey, 1987). The RPCA procedure is considered to be superior to the method based on a combination of geopotential height anomalies in the "centres of action", in that the teleconnection patterns identified are based on the entire flow field, and not just from height anomalies at a few select locations. Monthly data on the teleconnection indices go back to January 1950. We used mean winter (DJF) values of all the indices except the TNH, in which December and January data were used due to the absence of mean values for February. Specific features of the teleconnection patterns will be described below as we discuss their associations with Great Lakes ice cover. To facilitate further discussions, the positive phases of the Northern Hemisphere teleconnection indices are presented in Fig. 2.

To characterize ENSO events we used two indices: 1) the SOI, and 2) the Multivariate ENSO Index (MEI). The SOI was used in its standard form as the difference in SLP between Tahiti and Darwin. These data are also available from the CPC web site. The MEI (courtesy of K. Wolter) can be understood as a weighted normal of the main ENSO features contained in the following six variables: sea-level pressure, the east-west and north-south components of the surface wind, SST, SAT, and total amount of cloudiness. Positive (negative) values of the MEI represent the warm (cold) ENSO phase. The MEI is computed separately for each of twelve sliding bi-monthly seasons (Dec/Jan, Jan/Feb, ..., Nov/Dec). All seasonal values are standardized with respect to each season and to the 1950–1998 reference period. In our study we used only Dec/Jan values of the MEI. More details about this index are available in Wolter and Timlin (1998) and at the Climatic Diagnostics Center (CDC) web site[3].

Finally, to calculate composite maps for the WSI categories we used 700-hPa height and SST grid data over the Northern Hemisphere. These data are from the National Centers for Environmental Prediction/National Center for Atmospheric Research (NCEP/NCAR) reanalysis (Kalnay et al., 1996).

3 Method

The method used in this study is known as Classification and Regression Tree (CART). The core of this method is a binary tree-growing algorithm developed by

[2]http://www.cpc.noaa.gov/data/indices/tele_index.nh

[3]http://www.cdc.noaa.gov/ENSO/enso.mei_index.html

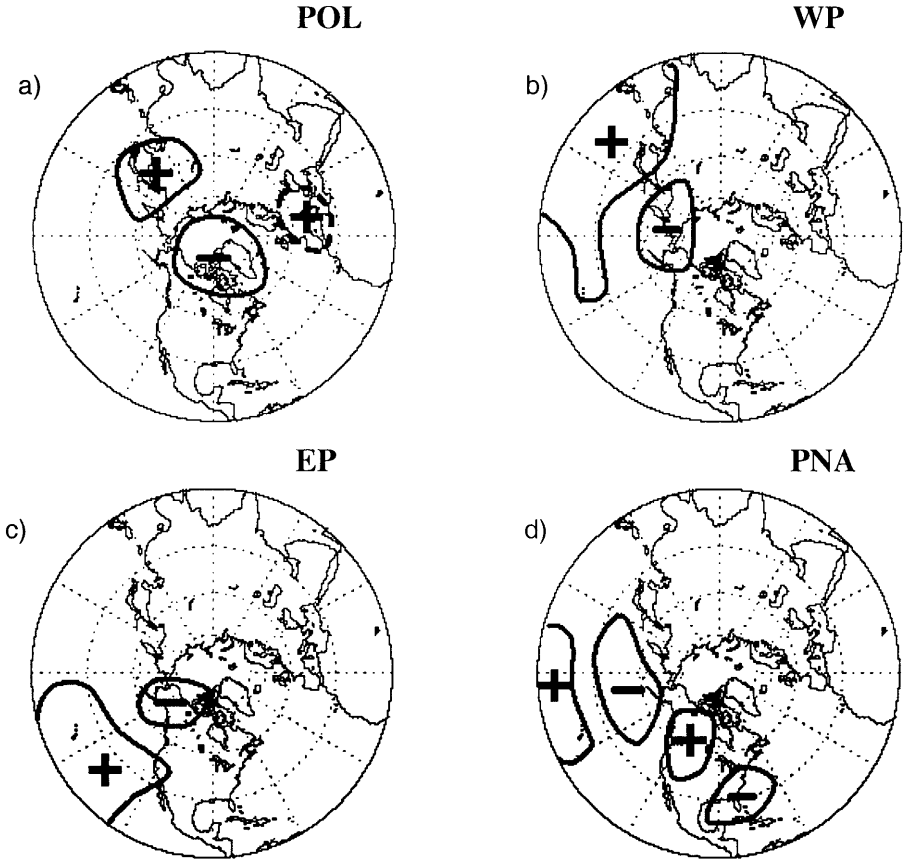

Fig. 2 Positive modes of the NH atmospheric teleconnection patterns including a) the POL pattern, b) the WP pattern, c) EP pattern, d) the PNA pattern, e) the TNH pattern, f) the NAO pattern, and g) the EA pattern. The NAO pattern is a surface pressure anomaly while all other patterns are 700-hPa height anomalies. Solid lines demarcate primary centres of action and dashed lines demarcate secondary centres of action.

Breiman et al. (1984). Tree-structured classification offers an interesting alternative to conventional methods such as discriminant analysis. A classification tree is an empirical rule for predicting the class of an object (the WSI in our case) from values of predictor variables (teleconnection indices). The CART is constructed by splitting subsets of the dataset using all predictor variables to create two child nodes repeatedly, beginning with the entire dataset.

The entire construction of a tree revolves around two major problems:

1. The selection of the splits, and
2. The decisions as to when to declare a node terminal or to continue splitting it.

The fundamental idea to resolve the first problem is to select each split of a subset

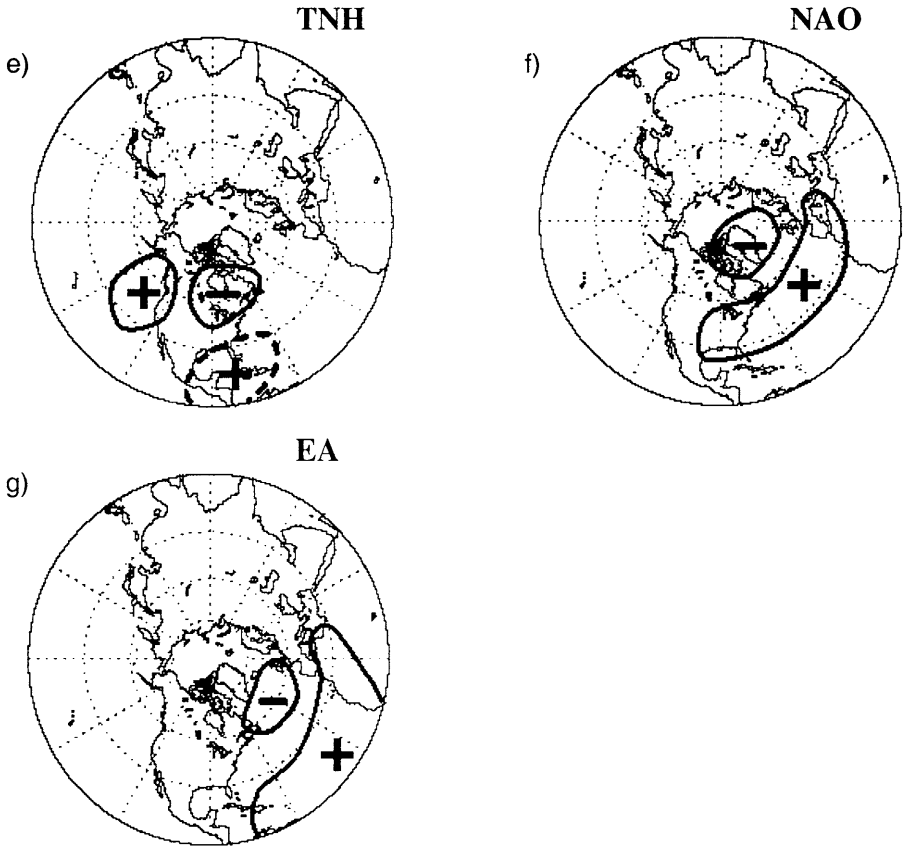

Fig. 2 (*Concluded*)

so that the data in each of the descendant subsets are "purer" than the data in the parent subset. In a completely pure node, all the cases belong to the same class of the target variable. For categorical target variables, the most popular indices to measure impurity are Gini and twoing described in detail by Breiman et al. (1984). They noted, however, that within a wide range of splitting criteria, the properties of the final tree are surprisingly insensitive to the choice of impurity measure, especially at the upper levels of the tree. In our analysis we used the Gini index of impurity g, which can be defined for node t as

$$g(t) = 1 - \sum_i \sum_{j \neq i} p(j|t)p(i|t),$$

where i and j are classes of the target variable, and $p(j|t)$ is the probability of class j in node t. This can also be written as

$$g(t) = 1 - \sum_j p^2(j|t).$$

When the cases are evenly distributed across the classes, the Gini index takes its maximum value of $1 - 1/k$, where k is the number of classes for the target variable. When all cases in the node belong to the same class, the Gini index equals 0. To measure a decrease in impurity for split s, CART uses a criterion function defined as

$$\Phi(s, t) = g(t) - p_L g(t_L) - p_R g(t_R),$$

where p_L is the proportion of cases in t sent to the left child node, and p_R is the proportion sent to the right child node. The split s is chosen to maximize the value of $\Phi(s, t)$. This value, weighted by the proportion of all cases in node t, is the value reported as "improvement" in the tree.

The process of splitting repeats recursively until one of the stopping rules is triggered, for example when the depth of the tree has reached its prespecified maximum value or the maximum decrease in impurity is less than a prespecified value. There are many situations, however, when these stopping rules, do not work well. Depending on the threshold, the splitting may either stop too soon at some terminal nodes or continue too far in other parts of the tree. Breiman et al. (1984) offered another approach to this problem. Instead of using stopping rules they suggest continuing the splitting until all terminal nodes are very small, resulting in a large tree, and then selectively pruning (recombining) this large tree upward. In our analysis we manually controlled the growth of each branch of the tree. We stopped when the number of observations in the terminal node became too small or when further splitting had no meaningful physical interpretation. Because of the relatively small sample size of our data, we never grew our trees more than three levels tall.

The CART algorithm we used (The AnswerTree™ 2.0 User's Guide, 1998) allows the user to change interactively the configuration of an automatically grown tree. This makes sense because the tree procedure is only one-step optimal and not overall optimal. Often two or more variables may have almost the same goodness of split, and choosing the "best" one may mask the effect of the others. An ability to interactively control the process of a tree construction and experiment with other variables is important in exploratory data analysis.

The CART method has a number of advantages over other classification methods:

- It is extremely robust with respect to outliers, that is the data that significantly differ from the rest of the data in the sample. This feature is similar to the robustness property of medians. If, for example, among N values of the PNA index in the learning set there is one that is much lower or higher than the others, it still will have weight $1/N$. When the program evaluates a split on the PNA, it essentially counts how many cases of each class go right or left, not taking into account the values of the index.
- Another frequently occurring error is mislabelling of a few cases in the learning set, for example assigning a warm category to a winter that was actually cold.

This can have a disastrous effect on linear discrimination, but the CART method can handle this situation fairly well. Again, since CART weighs each point as 1/*N*, the results are not appreciably affected by a few mislabelled points.

- CART makes powerful use of conditional information in handling nonhomogeneous information. This is particularly important for the Great Lakes region because, as shown by Hoerling et al. (1997), the reaction of this region to ENSO events appears to be substantially nonlinear.
- The tree-structured output of the CART procedure provides easily understood and interpreted information regarding a relationship between the target variable and its predictors. This information can also be presented as a set of IF-THEN rules, that is, in a form close to our natural language. These classification rules are nearly always found to make physical sense (Burrows and Assel, 1992).

CART is a relatively new approach to classification and regression problems in atmospheric sciences, and there are just a few published studies where it was applied. Rodionov (1994) used a procedure similar to CART to examine teleconnections for water level in the Caspian Sea. He found that fluctuations in water level at different timescales have a strong association with the state of the NAO. Zorita et al. (1995) applied the CART technique to classify observed daily SLP fields into weather types that are most strongly associated with the presence/absence of rainfall at selected index stations in the Columbia River basin and middle-Atlantic regions. Then they used the circulation types identified by CART to generate daily precipitation time series at individual stations and compared their statistical properties with the General Circulation Model (GCM) output.

In one case, the CART technique was applied directly to ice cover on the Great Lakes. Burrows and Assel (1992) developed a tree-based statistical regression model for predicting daily ice cover on lakes Superior and Erie. Potential predictors were designed from three considerations: characteristics of winter airmasses and wind conditions affecting a basin, the solar radiation cycle, and daily predictions from a freezing-degree-day model (Assel, 1990). It was found that the airmass indicator predictors were the overall most important predictors of ice for both lakes. The error of the ice cover percentage prediction for Lake Superior was estimated to be about 10–20%, and about 15–20% for Lake Erie. This is a respectable result, considering the error in the ice cover observations themselves is about 10%.

Unlike Burrows and Assel's (1992) work, the present work deals with the interannual timescale and with diagnosis rather than prediction of winter conditions in the Great Lakes basin. Its goal is to produce tree-based classifiers that will help to determine atmospheric circulation patterns characteristic of warm, normal and cold categories of the WSI.

4 Classification Trees and Rules

A classification tree with the lowest misclassification error among all those that were grown with a maximum depth of three levels is presented in Fig. 3. It correctly classifies 39 out of 49 cases (80%), so that the rate of misclassification (or risk esti-

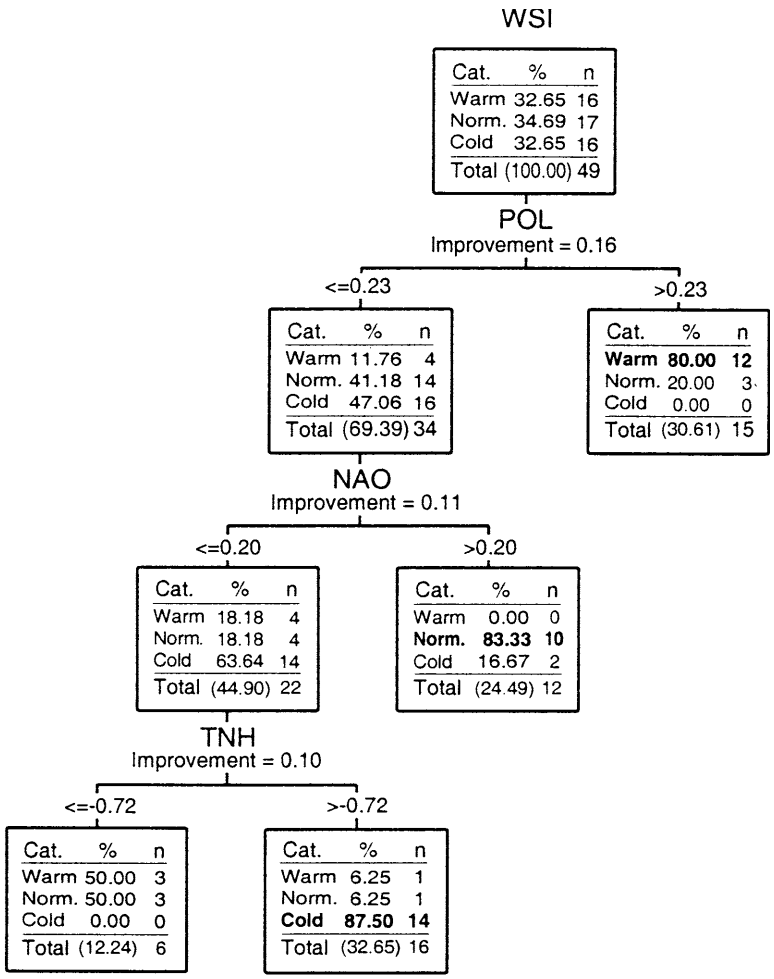

Fig. 3 A classification tree with the lowest risk estimate (boldface classes are discussed in the text).

mate) is $1 - 0.8 = 0.2$ (Table 1). Note that the misclassification mostly occurs to the neighbouring class. In fact, there was only one case when a warm winter (1955) was classified as a cold winter.

The best predictor in the root node of the tree is the POL index. It provides the highest improvement score of 0.16 among all the indices used in this study. The splitting point for this index is 0.23, that is, those winters with the POL index equal to or less than 0.23 go to the left and those with the POL greater than 0.23 go to the right. The overwhelming majority of winters in the right node (12 out of 15, or 80%) are warm, so that the purity of this terminal node is very high, and we can classify it as

TABLE 1. Misclassification matrix for the tree presented in Fig. 3.

	Actual Category			
Predicted category	Cold	Normal	Warm	Total
Cold	14	1	1	16
Normal	2	10	0	12
Warm	0	6	15	21
Total	16	17	16	49

Risk Estimate 0.20

'warm.' This branch of the tree can be written in the form of an IF-THEN rule:

```
Rule W1:
IF POL > 0.23,
THEN winter is warm (12/3/0).
```

In parentheses are numbers of warm, normal and cold winters correspondingly. This rule correctly classifies three fourths of all warm winters in the Great Lakes basin for the period 1950–1998. It is important to underscore that there were no cold winters during this period if the POL index was greater than 0.23.

When the POL index is less than or equal to 0.23, winters tend to be either normal or cold. The next step, which involves the NAO index, creates a group of predominantly normal winters. The rule that describes this group is

```
Rule N:
IF POL ≤ 0.23 & NAO > 0.2,
THEN winter is normal (0/10/2).
```

The final split in this tree is made on the TNH index. When this index is not strongly negative (TNH > –0.72), we have a group of 16 years comprised mostly of cold winters. The rule for this group of winters is

```
Rule C1:
IF POL ≤ 0.23 & NAO ≤ 0.20 & TNH > -0.72,
THEN winter is cold (1/1/14).
```

Despite a relatively complex logical condition in the premise of this rule, it classifies 88% (14 out of 16) of cold winters during the 1950–1998 period. In qualitative terms this rule indicates that if both the POL and NAO indices are not substantially positive and the TNH index is not in its extremely negative phase, the winter in the Great Lakes basin will most likely be colder than normal. The left child node after the split on TNH contains three warm and three normal winters. Both the purity of

the node and small number of cases do not allow us to classify this group as a separate circulation pattern. (To calculate the estimated risk in Table 1 we assigned a "warm" class to this terminal node.)

In exploratory data analysis it is important to look at the data from a number of different viewpoints. As shown in Section 3, if a predictor is not used in the tree, it does not necessarily mean that it has little association with the target variable. The truth may be that its effect was masked by other predictors. We found it important to experiment with other predictors that had lesser, but still substantial improvement score. The trees built with these other predictors provided valuable additional information emphasizing different aspects of the relationship between the severity of winters in the Great Lakes basin and large-scale atmospheric circulation.

The next best predictor after the POL index in the root node was the WP index. Those winters when this index is greater than 0.18 tend to be warmer than normal. Out of 17 winters that satisfied this condition during the 1950–1998 period, 11 (or 65% of this class) were warm, 5 normal and only 1 cold. In 8 of these 11 warm winters the POL index is also greater than 0.23, that is, there is a certain overlap with rule W1. These two indices, however, significantly complement each other: in 15 out of 16 warm winters either the POL index was greater than 0.23 or the WP index was greater than 0.18.

The third highest improvement score at the root node belongs to the MEI index. When this index is greater than 0.8 (indicating strong El Niño conditions) we have a group of 10 winters, 7 of which are warm and 3 are normal. These warm winters are 1958, 1964, 1983, 1987, 1992, 1995 and 1998. All of them are also characterized by positive values of POL, WP and PNA indices.

We also experimented with the PNA teleconnection index. It had almost the same improvement score in the root node as the MEI index. The split of the root node into child nodes using the PNA index was not, however, very impressive in terms of separating the extreme winter classes. Nevertheless, we continued to grow the tree and found two interesting combinations of the PNA with other indices:

```
Rule C2:
IF PNA ≤ -0.20 & TNH > -0.05,
THEN winter is cold (3/4/7).

Rule C3:
IF PNA > -0.2 & POL > 0.22,
THEN winter is cold (3/3/9).
```

Both of these rules describe an atmospheric circulation associated with predominantly cold winters in the Great Lakes basin. While the purity of the corresponding terminal nodes of the tree is not high, the composite maps for these groups of years, as we will see in Section 6, provide an important insight into the mechanism of atmospheric control of winter temperatures in the basin.

The last index we would like to mention here is the TNH. The classification tree

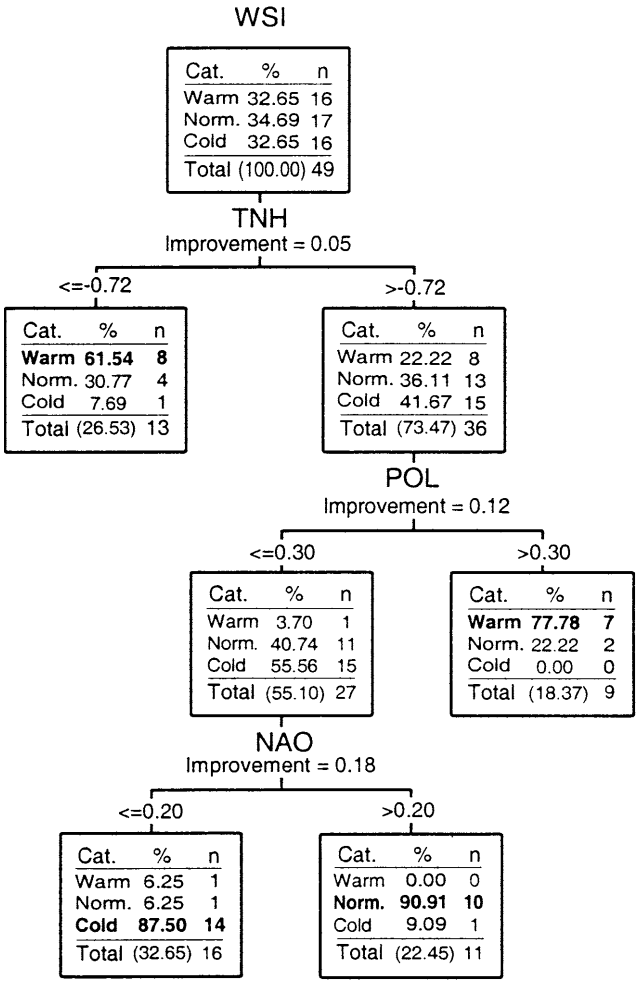

Fig. 4 A classification tree with the first split made on the TNH index.

with the split of the root node based on this index is presented in Fig. 4. Despite the low improvement score at the root node the overall risk estimate for this tree is only marginally higher than for the tree in Fig. 3. The teleconnection indices used in these two trees are the same. The splitting points are also either the same or very close. The terminal nodes for cold and normal winters on both trees contain practically the same years. The important difference between these two trees is in how they split warm winters. While the majority of warm winters in the tree in Fig. 3 are grouped in one terminal node, the tree in Fig. 4 has two terminal nodes with an approximately equal number of warm winters. These nodes can be described as follows:

```
Rule W2:
IF TNH ≤ -0.72,
THEN winter is warm (8/4/1).

Rule W3:
IF TNH > -0.72 & POL > 0.30,
THEN winter is warm (7/2/0).
```

The type of circulation described by rule W3 can be considered as a sub-type of W1, for which the TNH index is greater than –0.72. The type W2, however, is substantially different from both W1 and W3 . As we will see in Section 6, these three types help to better understand the dynamics of large-scale atmospheric circulation associated with warm winters in the Great Lakes basin. Before we proceed with the description of types of atmospheric circulation, let us consider the relationship between the WSI and some individual teleconnection indices that are major components of those types of atmospheric circulation.

5 Role of individual teleconnection indices

a *The POL index*

The POL index (Fig. 2a) was the most important teleconnection index for classification of warm winters. Its improvement score is much higher than for any other teleconnection index. Even if it is not chosen at the first split, it often emerges at the lower levels of the trees. This indicates that the POL index has some unique features that cannot be masked by other indices.

The POL pattern appears only in winter and is one of the most prominent modes of low-frequency variability during this season. The POL index reflects major changes in the strength of the circumpolar circulation. During the positive phase of this pattern when geopotential height anomalies in its main centre over the polar region are negative (Fig. 2a) the circumpolar vortex is strengthened, and the atmospheric circulation over the entire Northern Hemisphere is predominantly zonal. A prolonged positive phase of the POL index started in 1989 and continued through the 1990s. This may, at least partly, explain an increased frequency of warm winters during this period (Fig. 1).

The correlation coefficient between the POL index and the WSI is $r = –0.39$, which is significant at the 95% level, but not as high as one could expect based on its role in the construction of the decision trees. What reduces the correlation coefficient is an apparent asymmetry of the relationship between the POL index and the WSI. Although the POL index effectively classifies the majority of warm winters, it is not nearly as good at classification of cold winters. This asymmetry appears to reflect the fact that the distribution of SAT anomalies during meridional circulation is not, strictly speaking, exactly opposite to that during zonal circulation. True, upper atmospheric ridges and troughs tend to develop over particular regions, determined by the distribution of oceans and continents as well as mountain chains. Since

the meridional and zonal types of circulation are considered as an amplification and damping of those ridges and troughs, the distribution of SAT anomalies during one type of circulation is, to a first approximation, opposite to that during the other type of circulation. Upper ridges and troughs, however, can form over other regions as well, and that may completely change the distribution of SAT anomalies. Therefore, two winters with a generally meridional type of circulation may have significantly different SAT anomalies in the Great Lakes basin.

b *The WP Index*

Another teleconnection index that is important to understanding specifics of large-scale atmospheric circulation during warm winters in the Great Lakes basin is the WP index. Although the correlation coefficient between the POL and WP indices is not significant, the latter is almost as effective in classifying warm winters as the former. The WP pattern is a primary mode of low-frequency variability over the North Pacific. A positive phase of this pattern is characterized by a north-south dipole of 700-hPa height anomalies, with negative anomalies over the Berring Sea and positive anomalies in the moderate latitudes of the western and central North Pacific (Fig. 2b). This means that strengthening of the zonal flow over a large portion of the North Pacific will likely lead to a mild winter in the Great Lakes basin.

A positive phase of the WP index is also associated with positive SAT and SST anomalies in the Kuroshio region. The correlation coefficients between the WP index and SST and SAT in the Kuroshio region, south of Japan, calculated for the period 1958–1998 using NCEP/NCAR reanalysis data (Kalnay et al., 1996), exceed 0.5 and 0.8 respectively. (Correlation coefficients between WP, as well as other teleconnection indices and climatic variables in grid points over the globe, were provided by the NOAA-Cooperative Institute for Research in Environmental Sciences (NOAA-CIRES) Climate Diagnostic Center from http://www.cdc.noaa.gov/.) Chen and Reiter (1986) have examined the relationship between SST in the Kuroshio region and SAT over North America. They found that the correlation between these two variables reaches its maximum in the Great Lakes region and is more significant in winter ($r > 0.55$, significant at the 99.9% level). It remains equally strong for SAT over the Great Lakes, lagging SST in the Kuroshio by one month.

c *The MEI*

This study has confirmed our previous finding (Assel and Rodionov, 1998) of a strong association between warm winters in the Great Lakes basin and El Niño events. It also reveals, however, an obvious asymmetry in the relationship between the MEI and WSI. Although there is a tendency for cold winters to occur more frequently as the MEI decreases, there is no clear separation of this category when the MEI is negative. This suggests that the reaction of winter temperatures in the Great Lakes basin to La Niña events is less strong and/or less consistent than to El Niño events. A similar asymmetry (nonlinearity) was noted in a number of recent studies of ENSO effect on seasonal precipitation, surface temperature, and teleconnection

patterns (Zhang et al., 1996; Livezey et al., 1997; Hoerling et al., 1997; Mo et al., 1998; Montroy et al., 1998). For example, Mo et al. (1998) have demonstrated that the WP response to the ENSO signal is stronger during El Niño events than during La Niña events. Hoerling et al. (1997) have presented composite wintertime (DJF) SAT anomaly maps over North America for El Niño and La Niña. Each composite map is an average of nine cold or warm events between 1950 and 1996. The maximum warm temperature, anomaly during El Niño is located near Lake Superior, but this resides at the zero temperature anomaly line of the La Niña composite, and the two maps are nearly in quadrature. The nonlinear component of the SAT anomalies, as estimated by Hoerling et al. (1997) reaches its maximum over the Great Lakes, suggesting that this is the area where much can be gained by treating the North American climate response to warm and cold events separately.

d *The PNA Index*

Numerous studies have documented that the PNA pattern is the dominant extratropical response to ENSO forcing affecting the circulation over North America (Horel and Wallace, 1981; Livezey and Mo, 1987; Molteni and Tibaldi, 1990; Renshaw et al., 1998). In fact, all seven strong El Niño events mentioned in the previous section, for which the MEI index was greater than 0.80, were accompanied by a positive PNA index. Therefore, it was somewhat surprising to find that the probability of cold and warm winters is approximately the same for positive and negative values of the PNA index. Ironically, both the coldest (1976/77) and the warmest (1997/98) winters on the Great Lakes during the 1950–1998 period were El Niño winters with the highest and second highest positive PNA indices respectively (Rodionov and Assel, 1999).

It is known that great distortions of the PNA pattern are possible, to the extent that the resulting anomaly pattern only vaguely (if at all) resembles the PNA configuration (Yarnal and Diaz, 1986; Kushnir and Wallace, 1989; Keables, 1992). Often these distortions are due to the influence of other teleconnection patterns. Barnston and Livezey (1987), for example, have shown that the PNA pattern can blend with the TNH pattern (most often during January-February-March and February-March-April seasons) and form a pattern with the features centred in between these two. In fact, in both the winters of 1982/83 and 1997/98 the TNH index was strongly negative, so that 700-hPa height anomalies were positive all over northern North America. In contrast, in the winter of 1976/77, the TNH index was positive, and that corresponded to a deep trough over the eastern part of the continent. Shabbar and Khandekar (1996) found that for some ENSO winters a transition occurs from the PNA pattern in early winter to the TNH pattern by the following late winter through early spring.

A significant variability in the spatial configuration of the PNA anomaly centres was noted in some other studies. Thus, Keables (1992) identified three types of the PNA-like circulation. Two of these types are associated with predominantly negative SAT anomalies in the Great Lakes region. The third one, which resembles the

TNH pattern, is associated with positive SAT anomalies in the Great Lakes region. To test the robustness of the PNA pattern, Kushnir and Wallace (1989) repeated a rotated principal component analysis for two periods, 1947–1965 and 1966–1985. They found that the primary centre of action over the North Pacific shifted 15 degrees eastward and 5 degrees southward from the first period to the second. In another experiment, they used the oblique rotation (instead of the conventional orthogonal rotation) of the first 15 eigenvectors of the correlation matrix for the entire 38-year period. The first two principal components on the interannual time-scale resembled the PNA pattern, but were nearly in quadrature with one another.

It is also important to note that some areas are very sensitive to relatively minor changes in the structure of the PNA. Yarnal and Diaz (1986) showed for the west coast of North America that a shift of just a few hundred kilometres in the zero-line of the 700-hPa height anomaly field represents a repositioning of the mean storm track and a change from an abnormally dry anticyclonic regime to exceedingly wet cyclonic conditions, and vice versa. The same appears to be true for the Great Lakes. Brinkman (1999) demonstrated how seemingly small changes in 700-hPa height anomalies east of Lake Superior might result in vastly different surface conditions.

Thus, the geographical position of the Great Lakes relative to the PNA pattern (too close to the nodal point of this standing oscillation), instability of the pattern itself, and the inability of the PNA index to characterize unambiguously atmospheric circulation does not make this index a good classifier for the WSI. Still the PNA index can be useful if it is combined with other teleconnection indices. As we found, the PNA combined with the POL and TNH indices are able to characterize types of atmospheric circulation associated with cold winters. These and other types of atmospheric circulation for cold, normal and warm winters are considered in the next section.

6 Types of atmospheric circulation

Table 2 summarizes the types of atmospheric circulation for warm, normal and cold winters. The description of these types is given in terms of teleconnection indices. Here we further explore these types using composite maps of 700-hPa height and SAT anomalies. Winters that comprise each of the composites are listed in Table 3. It is important to note that the classification we use here is hierarchical. Type W1 represents the most general features of atmospheric circulation for warm winters. Its composite map consists of most winters of W2 and W3 types, except those indicated (Table 3). Likewise, type C1 is superior to types C2 and C3. The only winter of an extreme category that remains unclassified is the warm winter of 1955.

a *Warm Winters*

1 TYPE W1

Composite maps of 700-hPa height and SAT anomalies for type W1 are presented in Figs 5a and 5b respectively. As Fig. 5a demonstrates, atmospheric circulation over the Northern Hemisphere is dominated by strong negative 700-hPa height anomalies

TABLE 2. Types of atmospheric circulation for warm, normal and cold winters in the Great Lakes basin and their description in terms of teleconnection indices.

Winter	Circulation Type	Description
Warm	W1	POL > 0.23
	W2	TNH < –0.72
	W3	TNH > –0.72 and POL > 0.30
Normal	N	POL ≤ 0.23 and NAO > 0.2
Cold	C1	POL ≤ 0.23 and NAO ≤ 0.20 and TNH > –0.72
	C2	PNA ≤ –0.20 and TNH > –0.05
	C3	PNA > –0.2 and POL > 0.22

TABLE 3. Classification of winters by types of atmospheric circulation

W1			C1	
W2	W3	N	C2	C3
1953*	1954	1950	1959	1963
1958	**1964**	1951	1962	1968
1960*	1975	1952	1965	1970
1983	1976	1957	1971	1977
1987*	1989	1961	1972	1978
1992	1991	1967	1979	1981†
1995	1993	**1973**	1982	1986
1998		1974		1994†
		1984		1996
		1988		

*Winters not included in W1
†Winters not included in C1
Winters with strong El Niño events (the MEI index is greater than 0.8) are bolded.

over the polar region and northern parts of the North Pacific, North Atlantic and Russia. Positive 700-hPa height anomalies occupy the middle latitudes with the highest anomalies over western Europe. This distribution of the height anomalies indicates strong westerly winds over the entire Northern Hemisphere (NH) and particularly over the Atlantic sector. The latter carries a clear signature of the positive phase of the NAO. Over the North Pacific a positive mode of the WP pattern is also noticeable.

It is important to note the existence of positive height anomalies over the Great Lakes region. Although the magnitude of these anomalies is not very high, their sign is very persistent, being present in the region almost every warm winter. As shown by Assel and Rodionov (1998) the correlation coefficient between ice cover in the Great Lakes and 700-hPa height in the area over and to the north of the Great Lakes basin is significant at the 95% level. The absolute values of the correlation coefficient exceed 0.6 for lakes Superior and Huron. During a zonal type of atmospheric circulation over the Northern Hemisphere when amplitudes of planetary waves are

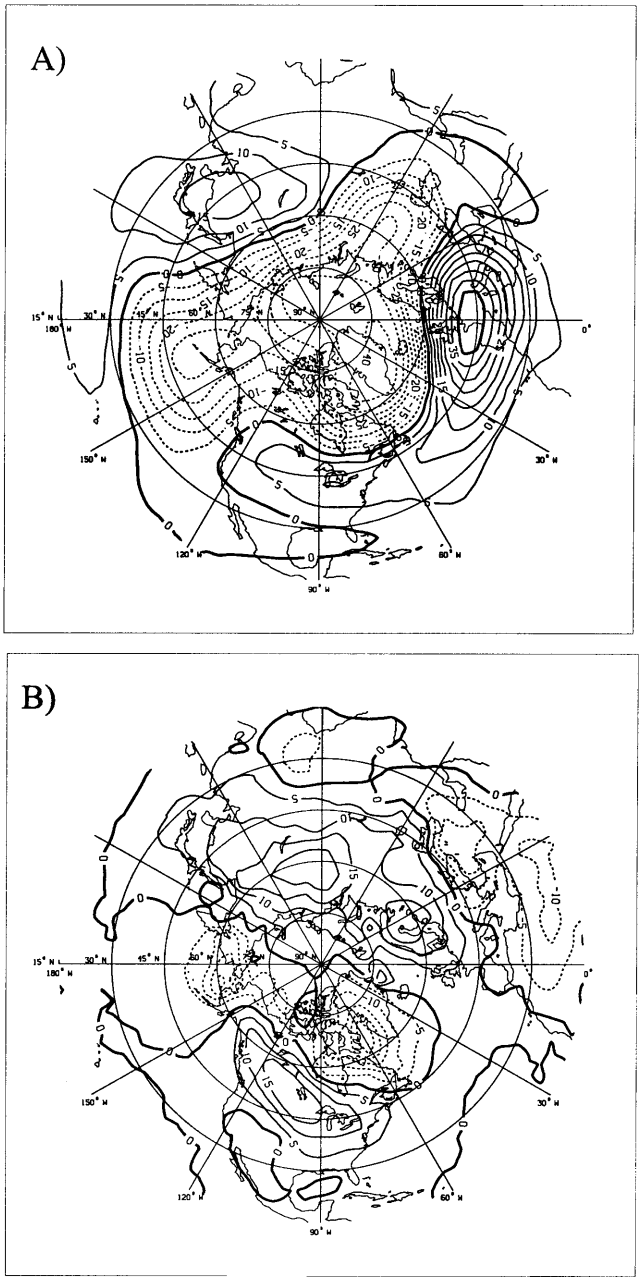

Fig. 5 Composite maps of a) 700-hPa height anomalies (in metres) and b) SAT anomalies (in °C × 10) for W1 type of atmospheric circulation. Anomalies are calculated as deviations from the 1950–1998 period.

relatively small, cold Arctic air is confined in the high latitudes. The positive 700-hPa height anomalies in the Great Lakes region are an indication that the climatological upper atmospheric trough over eastern North America is not developed, and outbreaks of cold Arctic air, are infrequent if not absent altogether.

The SAT anomalies associated with W1 (Fig. 5b) are mostly positive over central parts of North America, particularly in the area stretching from northwestern Canada to the eastern United States, completely covering the Great Lakes. The strongest negative SAT anomalies are located north of 60°N, from the Bering Sea to Greenland.

2 TYPE W2

A composite map of 700-hPa anomalies for W2 type (Fig. 6a) features a dipole with the negative centre over the eastern North Pacific and the positive one north of the Great Lakes. It represents a strongly negative phase of the TNH pattern. A comparison with the TNH pattern from the CPC (Fig. 2e) reveals that the North Pacific centre on the composite map is shifted about 15 degrees of longitude westward relative to its counterpart on the CPC's map and is closer to the negative North Pacific centre for the PNA (Fig. 2d). It is important to note that 6 out of 8 winters that comprise the composite (i.e., 1958, 1983, 1987, 1992, 1995 and 1998) are winters with strong El Niño events with the MEI greater than 0.8. Therefore, type W2 of atmospheric circulation also characterizes to some degree a response of extratropical circulation over the Northern Hemisphere to strong El Niño events.

The positive 700-hPa height anomaly centre north of the Great Lakes indicates a significant weakening of the Hudson Bay low. The jet stream loops southward over the eastern North Pacific and deviates significantly to the north of its typical position over the continent (Fig. 7a). Due to a broad southerly "anomalous" flow, winter SAT anomalies are positive over most of North America (Fig. 6b). Their spatial distribution is similar to that for W1 type (Fig. 5b), but their magnitudes, exceeding 3.0°C over central Canada, are noticeably higher. SAT anomalies over the Great Lakes basin are on the order of 1.5°C–2.5°C.

3 TYPE W3

Atmospheric circulation of W3 type represents a sub-type of W1 with a particularly strong zonal flow over the Northern Hemisphere (Fig. 8a). Geopotential height anomalies are on the order of –6 dam in the Polar region, which makes the circumpolar vortex more vigorous compared to W1 type. It is also more contracted over the Pacific sector and expanded southward over North America. The latter suggests a stronger than normal intensification of the Hudson Bay low. This is accompanied by suppressed cyclonic activity over the eastern North Pacific, which is characteristic of a positive phase of the TNH pattern (Fig. 2e). The overall distribution of 700-hPa height anomalies over the Pacific/North American sector is opposite to that for W2 type circulation (Fig. 6a). The polar jet stream is almost zonally oriented (Fig. 7b).

As with W1 and W2 type, the strongest negative SAT anomalies associated with

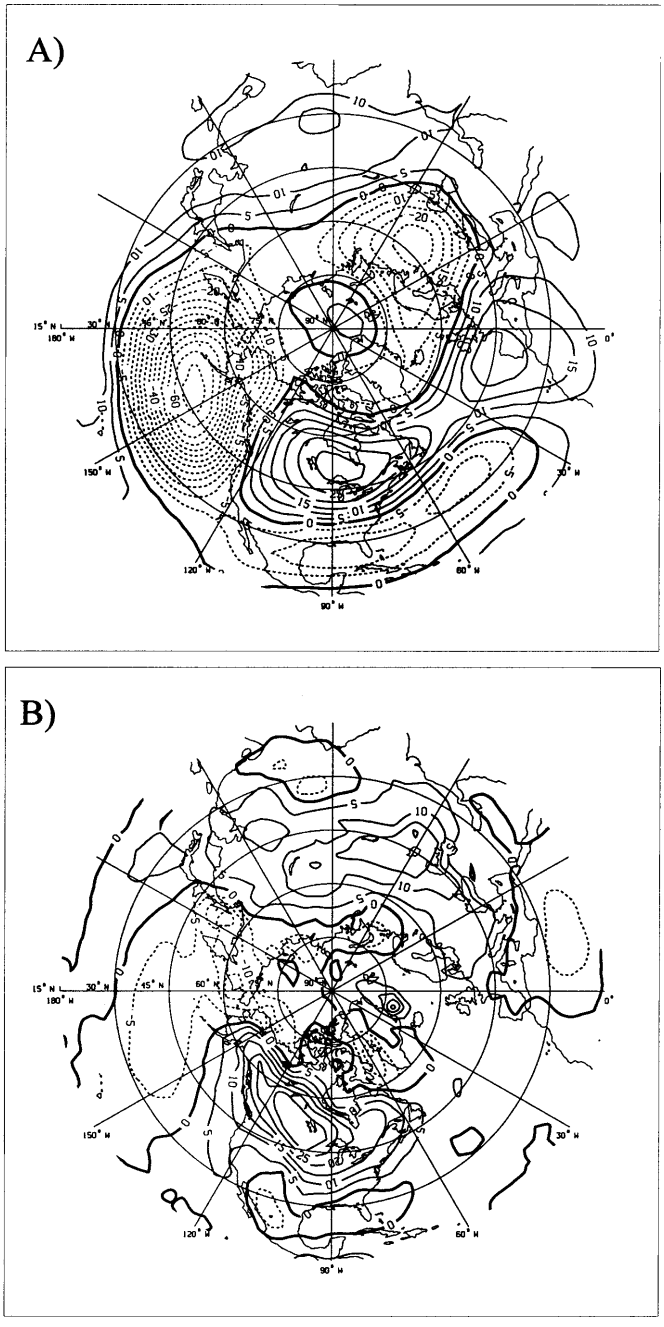

Fig. 6 Same as Fig. 5, except for W2 type.

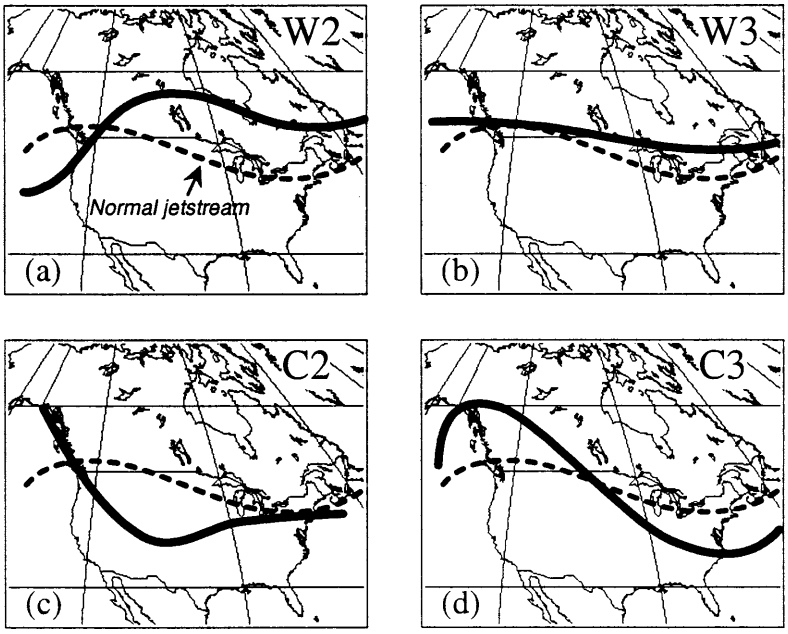

Fig. 7 A typical configuration of the polar jet stream during a) W2, b) W3, c) C2 and d) C3 types of atmospheric circulation.

W3 type (Fig. 8b) are in the high latitudes, with the centres over the Bering Sea and the Baffin Bay/Labrador Sea region. The latter is a signature of a positive, or "Greenland below" (Rogers and van Loon, 1979), phase of the NAO, when the Icelandic low is strong and an advection of cold Arctic air along its western periphery is enhanced. Negative SAT anomalies, however, are limited to eastern Canada. Further south and east they become positive, exceeding 0.5°C over the Great Lakes.

b *Normal Winters*

Normal winters usually occur when none of the extreme types of atmospheric circulation is well developed. Therefore, it is usually difficult to find something in common for normal winters. It was found, however, that for more than half of the normal winters in our analysis (10 out of 17) the characteristic feature is a combination of near-normal or negative POL index with a strongly positive NAO index (Table 2). Although this positive NAO mode is clearly recognizable on the 700-hPa composite map (Fig. 9a), the Icelandic low is shifted south compared to the standard NAO pattern in Fig. 2f, which is more characteristic of the EA pattern (Fig. 2g). Due to this shift, the zero line between the two North Atlantic centres of action crosses the Great Lakes.

The NAO signature is also clearly seen in the distribution of SAT anomalies (Fig. 9b). In general, this distribution is similar to that associated with W1 and W3 types of

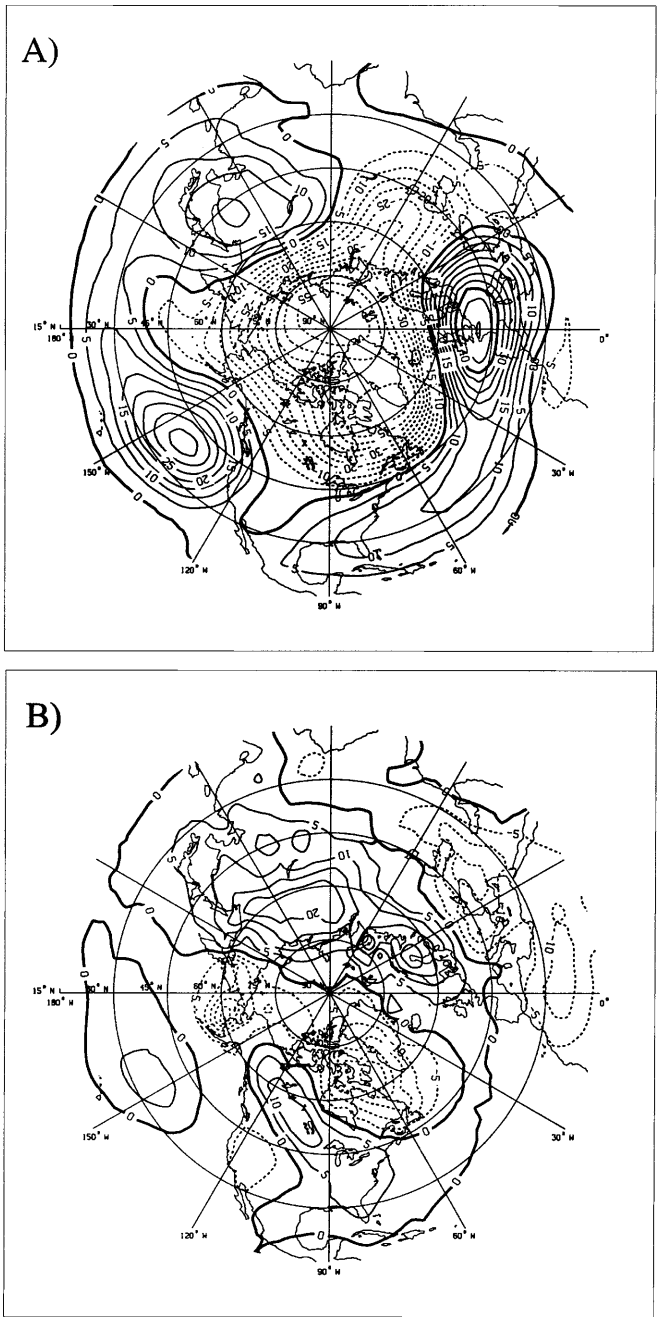

Fig. 8 Same as Fig. 5, except for W3 type.

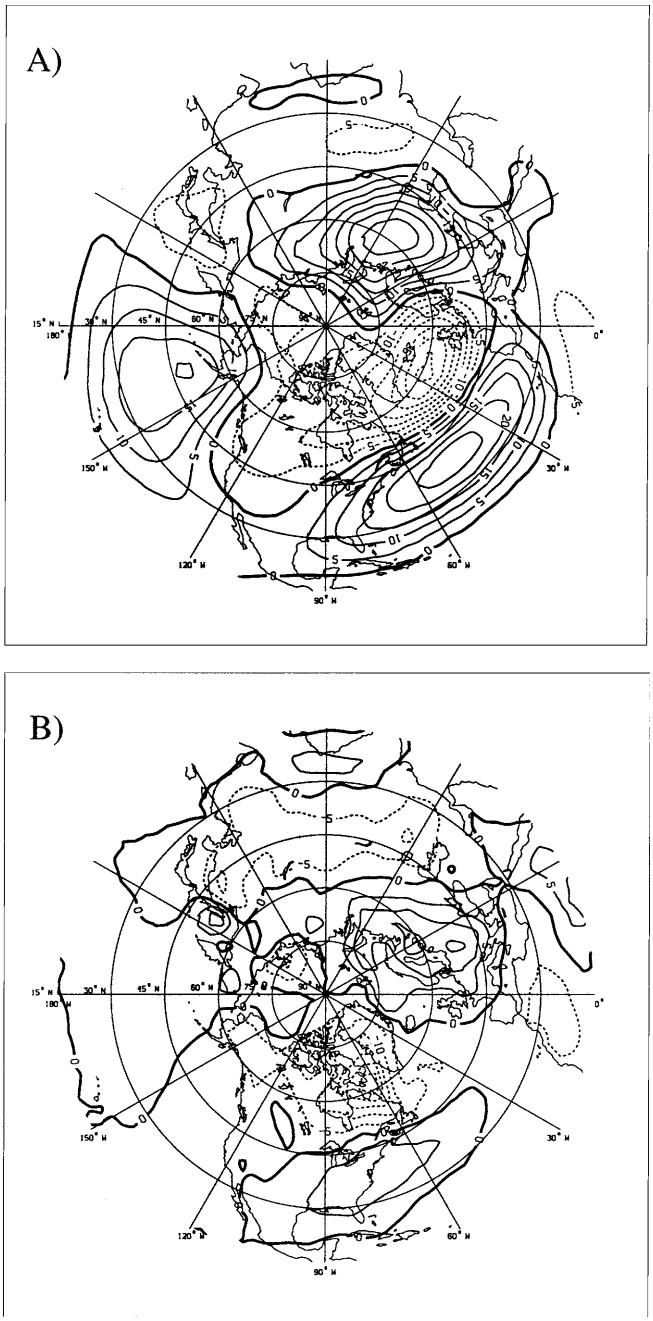

Fig. 9 Same as Fig. 5, except for N type.

circulation, but the cold anomaly over the western North Atlantic is shifted further south, so that the Great Lakes basin experiences near normal temperature conditions.

c *Cold Winters*

Unlike warm winters, which can often be successfully classified using just one teleconnection index, classification of cold winters is more complex and requires two or three teleconnection indices (Table 2). When these indices are combined they are usually in the phase that corresponds to the meridional rather than zonal circulation. As a result, all three types of atmospheric circulation, associated with cold winters (C1, C2 and C3), are meridional in nature.

1 TYPE C1

Atmospheric circulation of C1 type represents a combination of three teleconnection patterns: POL, NAO and TNH (Table 2). Elements of the first two can be easily recognized on the 700-hPa composite, map (Fig. 10a). Positive 700-hPa height anomalies in the high latitudes are characteristic of the negative phase of the POL. Strong positive anomalies over the Greenland-Iceland region and a belt of negative anomalies in the lower latitudes of the North Atlantic sector are a signature of the negative phase of the NAO. The TNH pattern can also be traced on this map. Positive anomalies in the Gulf of Alaska and negative anomalies in the Great Lakes region are indicative of a positive phase of this pattern. Overall, due to a predominance of positive anomalies in the high latitudes and negative anomalies in the mid-latitude belt, the zonal flow over the entire Northern Hemisphere is weakened. The reduction in the strength of the westerly winds is particularly significant over the North Atlantic sector.

The distribution of SAT anomalies associated with type C1 (Fig. 10b) is almost completely opposite to that for type W1 (Fig. 5b). Over North America, an area of negative SAT anomalies extends from northwestern Canada southeastward through the Great Lakes to the east coast of the United States. Over the North Atlantic sector, the distribution of SAT anomalies is in a typical "Greenland above" phase of the NAO (Van Loon and Rogers, 1978).

2 TYPE C2

Type C2 (Fig. 11a) is formed by a combination of negative PNA and positive TNH patterns (Table 2). The negative phase of the PNA is characterized by frequent troughing over the west of North America and ridging over the east. If, however, this is accompanied by a positive TNH pattern, which features a negative 700-hPa height anomaly north of the Great Lakes, the ridging on the east is suppressed (Fig. 7c). As seen in Fig. 11b, the strongest negative SAT anomaly under this pattern is over west-central Canada and the Great Lakes are located on the periphery of this anomaly. In this situation even the slightest variations in the atmospheric circulation pattern may have significant consequences for the Great Lakes. The probability of a cold winter is highest for Lake Superior and lowest for lakes Erie and Ontario.

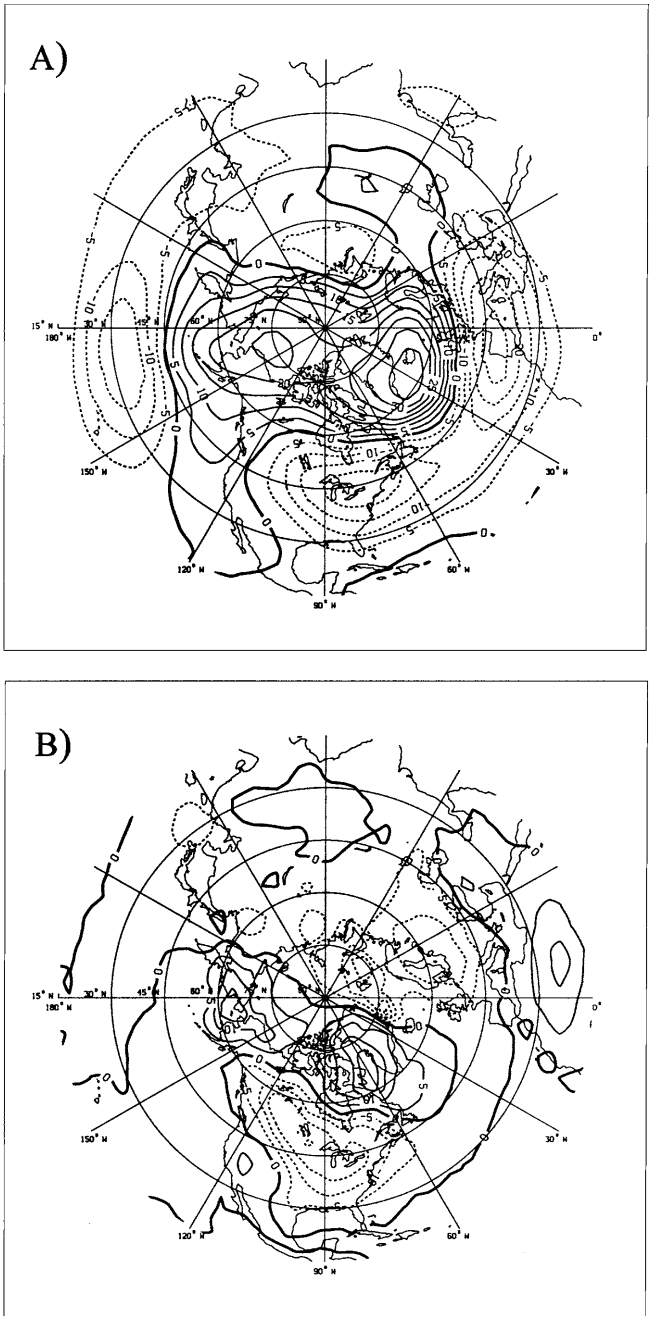

Fig. 10 Same as Fig. 5, except for C1 type.

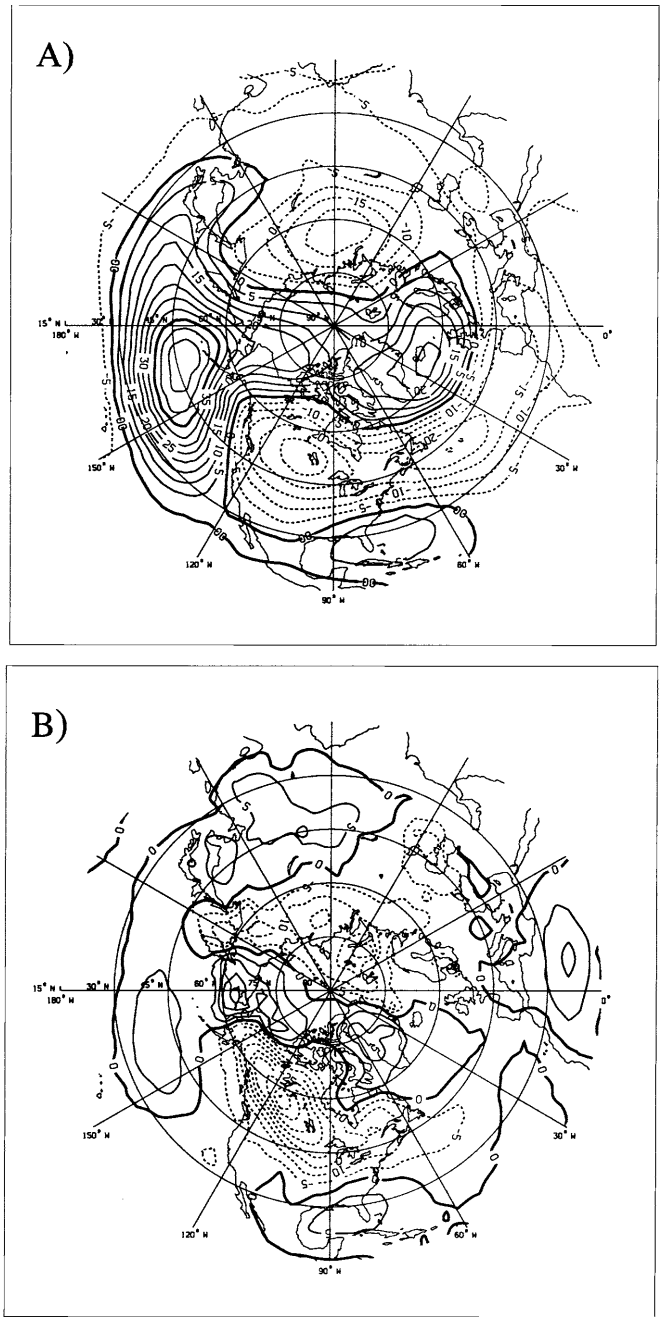

Fig. 11 Same as Fig. 5, except for C2 type.

3 TYPE C3

Type C3 represents a combination of the PNA and POL indices (Table 2). The distribution of 700-hPa anomalies under this type of circulation (Fig. 12a) is very similar to the classical PNA pattern (Wallace and Gutzler, 1981): a strong negative anomaly over the east-central North Pacific, positive anomaly over the Canadian Rockies, and negative anomaly over the U.S. east coast and adjacent waters. The ridge-trough system over North America (Fig. 7d) is well developed, so that cold Arctic air can easily reach the southeastern United States, where negative SAT anomalies are most significant (Fig. 12b). As was the case with type C2 the Great Lakes region is near the periphery of the negative anomaly, but in this case, the probability of a cold winter is higher for the lower lakes than for Lake Superior. During the coldest 3-year period of 1977–1979 (Fig. 1), the first two winters were of C3 type, while the third one was of C2 type.

7 Summary

Relationships between the Great Lakes WSI and winter atmospheric teleconnection patterns have been examined using the CART method. This method is particularly useful when a relationship between the target variable and predictors is not necessarily symmetric relative to the sign of the anomaly. Thus, we have found that warm winters in the Great Lakes basin are strongly associated with El Niño events in the equatorial Pacific. However, the association between cold winters and La Niña events is much weaker. This result is consistent with the maps of SAT anomalies during El Niño and La Niña events in Hoerling et al. (1997) who showed that the nonlinearity of the ENSO effect reaches its maximum in the Great Lakes region.

The CART method allowed us to reveal those teleconnection indices and their combinations that are most characteristic of warm, normal and cold winters. The single most important classifier for the WSI is the POL index. It effectively classifies 12 out of 15 warm winters during the 1950–1998 period. All 12 of these winters occurred when the POL index was greater than 0.23. It is important to emphasize that there were no cold winters when this condition was in place. As with ENSO, the effect of the POL index on the severity of winters in the Great Lakes basin is not symmetric. Consequently, the correlation coefficient (as a measure of strength of the linear relationships) between the POL and WSI is only moderately high.

By and large, warm winters tend to occur when the atmospheric circulation over the Northern Hemisphere is predominantly zonal (type W1). Within this type of circulation it is possible to distinguish two sub-types, W2 and W3. The majority of the warmest winters in the Great Lakes basin occurred during the W2 sub-type of circulation. This sub-type features enhanced cyclonic activity in the eastern North Pacific and a dome of high pressure over the continent, with the highest positive 700-hPa anomalies over and to the north of the Great Lakes. It represents a strong negative phase of the TNH pattern (the TNH index is less than –0.72), which is characterized by a broad southerly “anomalous” flow and above-normal temperatures almost everywhere in North America. Out of seven warm winters in the Great Lakes basin

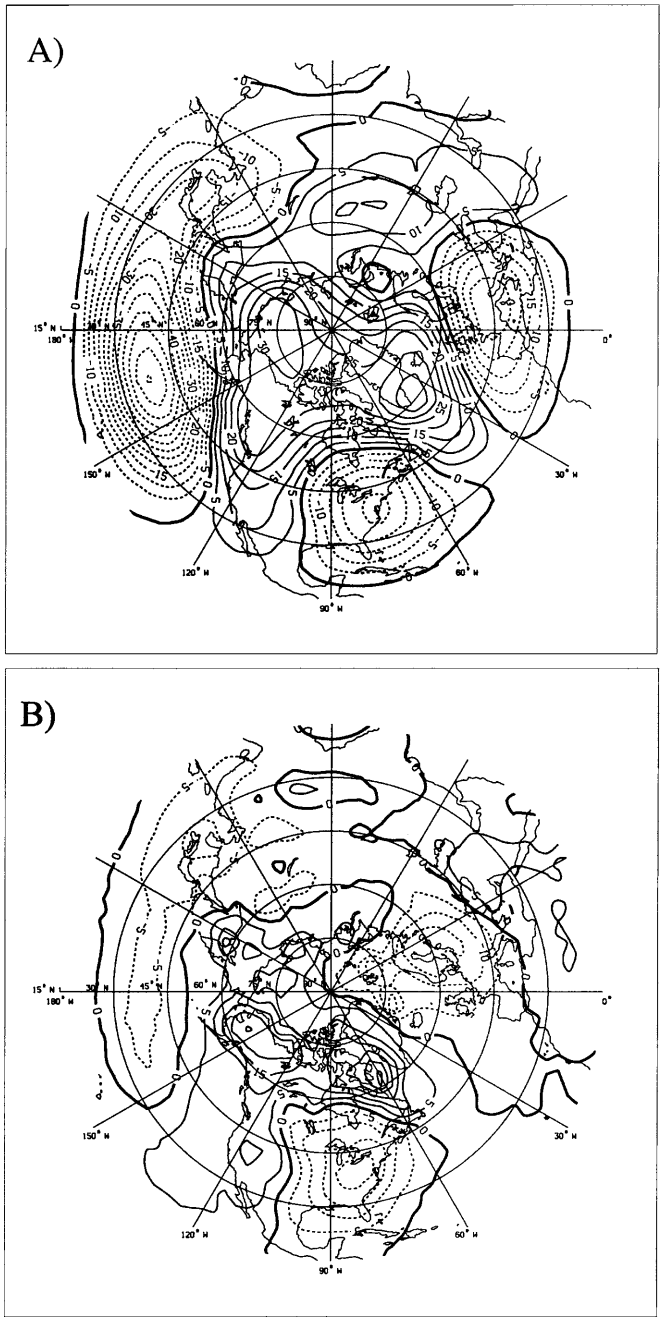

Fig. 12 Same as Fig. 5, except for C3 type.

that were accompanied by El Niño events, six winters were of W2 sub-type. During W3 sub-type of atmospheric circulation, the polar jet stream over North America assumes a near zonal direction. As a result, advection of cold Arctic air to the eastern part of North America is inhibited.

Although there is a clear tendency for cold winters to occur during years of meridional circulation over the Northern Hemisphere, the structure of the relationship between the WSI and atmospheric circulation for cold winters is more complex than that for warm winters. Usually it takes two or more teleconnection indices to classify cold winters successfully. The most common type of atmospheric circulation (C1) represents a combination of three teleconnection indices: POL $\leq$ 0.23 and NAO $\leq$ 0.20 and TNH > –0.72. These conditions were observed during 14 out of 16 (88%) cold winters, and there was only one warm winter that occurred under these conditions. There are two sub-types of atmospheric circulation (C2 and C3) that are based on subsets of cold winters and represent different aspects of atmospheric circulation leading to cold winters in the basin. Both sub-types involve the PNA index and show that cold winters may occur under both negative and positive phases of this pattern. When a negative phase of the PNA is accompanied by a positive phase of the TNH, the jet stream tends to loop southward over the western part of North America, but its northern excursion over the eastern part is suppressed. Since the major storm track lies south of the Great Lakes, the basin often finds itself behind the cold fronts of the passing cyclones. The strongest negative SAT anomalies are located over west-central Canada, extending toward the Great Lakes. In this situation the probability of a cold winter is higher for Lake Superior than for the lower Great Lakes. Sub-type C3 represents a combination of a positive phase of the PNA with normal or negative phases of the POL. The upper atmospheric ridge over the Rockies and the trough over eastern North America are amplified, which is accompanied by frequent outbreaks of cold Arctic air into the eastern part of the continent. The strongest negative anomalies are located south of the Great Lakes basin, so that the probability of a cold winter is higher for the lower Great Lakes than for Lake Superior.

Acknowledgements

We wish to thank Klaus Wolter for providing the MEI index. Sergei Rodionov's work on this project was supported by the National Research Council and the National Ice Center. This is GLERL contribution No. 1180. We wish to thank Dr. Brent Lofgren and Lynn Herceh of our staff and the four anonymous reviewers for their comments and suggestions.

References

ASSEL, R.A. 1990. An ice-cover climatology for Lake Erie and Lake Superior for the winter seasons 1897–98 to 1982–83. *Int. J. Climatol.* **10**: 731–748.

———. 1998. The 1997 ENSO event and implications for North American Laurentian Great Lakes Winter Severity and Ice Cover. *Geophys. Res. Letts.* **25**: 1031–1033.

——— and S. RODIONOV. 1998. Atmospheric teleconnections for annual maximum ice cover on the Laurentian Great Lakes. *Int. J. Climatol.* **18**: 425–442.

———; C.R. SNIDER and R. LAWRENCE. 1985. Comparison of 1983 Great Lakes winter weather and ice conditions with previous years. *Mon. Weather Rev.* **113**: 291–303.

———; J.E. JANOWIAK, D. BOYCE and S. YOUNG. 1996. Comparison of 1994 Great Lakes Winter Weather and Ice Conditions with Previous Years. *Bull. Am. Meteorol. Soc.* **77**: 71–88.

———; ———, ———, C. O'CONNORS, F.H. QUINN and D.C. NORTON. 2000. Laurentian Great Lakes ice and weather conditions for the 1998 El Niño winter. *Bull. Am. Meteorol. Soc.* **18**: 703–717.

BARNSTON, A.G. and R.E. LIVEZEY. 1987. Classification, seasonality and persistence of low-frequency atmospheric circulation patterns. *Mon. Weather Rev.* **115**: 1083–1126.

——— and Y. HE. 1996. Impacts of the NAO on U.S. and Canadian surface climate; Implications for seasonal predictions. *In*: Proc. 21st Annual Climate Diagnostics and Prediction Workshop, Huntsville, Alabama, 28 Oct. – 1 Nov. 1996. U.S. Dept. Commerce, NOAA/NWS/NCEP, pp. 34–37.

BREIMAN, L.; J.H. FRIEDMAN, R.A. OLSHEN and C.J. STONE. 1984. *Classification and Regression Trees.* Belmont, CA, Wadsworth, 358 pp.

BRINKMAN, W.A.R. 1999. Within-type variability of 700 hPa winter circulation patterns over the Lake Superior basin. *Int. J. Climatol.* **14**: 41–58.

BUNKERS, M.; J.R. MILLER, JR. and A.T. DEGAETANO. 1996. An Examination of El Niño-La Niña-Related Precipitation and Temperature Anomalies across the Northern Plains. *J. Clim.* **9**: 147–160.

BURROWS, W.R. and R.A. ASSEL. 1992. Use of CART for diagnostic and prediction problems in the atmospheric sciences. *In*: Proc. 12th Conference on Probability and Statistics in Atmospheric Sciences, 22–26 June 1992, Toronto, Canada, Am. Meteorol. Soc., Boston, U.S.A., pp. 161–166.

CHEN, L. and E.R. REITER. 1986. Sea surface temperature anomalies in the Kuroshio region and temperature anomalies over North America. *Meteorol. Atmos. Phys.* **35**: 1–9.

ESBENSEN, S.K. 1984. A comparison of intermonthly and interannual teleconnections in the 700 mb geopotential height field during the Northern Hemisphere winter. *Mon. Weather Rev.* **112**: 2016–2032.

HOERLING, M.P.; A. KUMAR and M. ZHONG. 1997. El Niño, La Niña, and the nonlinearity of their teleconnections. *J. Clim.* **10**: 1769–1786.

HOREL, J. and J.M. WALLACE. 1981. Planetary-scale atmospheric phenomena associated with the Southern Oscillation. *Mon. Weather Rev.* **109**: 813–829.

KALNAY, E.; M. KANAMITSU, R. KISTLER, W. COLLINS, D. DEAVEN, L. GANDIN, M. IREDELL, S. SAHA, G. WHITE, J. WOOLLEN, Y. ZHU, M. CHELLIAH, W. EBISUZAKI, W. HIGGINS, J. JANOWIAK, K.C. MO, C. ROPELEWSKI, J. WANG, A. LEETMAA, R. REYNOLDS, R. JENNE and D. JOSEPH. 1996. The NCEP/NCAR Reanalysis 40-year Project. *Bull. Am. Meteorol. Soc.* **77**: 437–471.

KEABLES, M.J. 1992. Spatial variability of midtropospheric circulation patterns and associated surface climate in the United States during ENSO winters. *Phys. Geog.* **13**: 331–348.

KUSHNIR, Y. and J.M. WALLACE. 1989. Low-frequency variability in the Northern Hemisphere winter: Geographical distribution, structure and time-scales. *J. Atm. Sci.* **46**: 3122–3142.

LAU, N.C. and M.J. NATH. 1990. A general circulation model study of the atmospheric response to extratropical SST anomalies observed in 1950–1979. *J. Clim.* **3**: 965–989.

LEATHERS D.J. and M.A. PALECKI. 1992. The Pacific/North American teleconnection pattern and United States climate. Part II. Temporal characteristics and index specification. *J. Clim.* **5**: 707–716.

———; B. YARNAL and M.A. PALECKI. 1991. The Pacific/North American teleconnection pattern and United States climate. Part I: Regional temperature and precipitation associations. *J. Clim.* **4**: 517–528.

LIVEZEY, R.E. and K.S. MO. 1987. Relationships between monthly mean Northern Hemisphere circulation patterns and proxies for tropical convection. *Mon. Weather Rev.* **115**: 3115–3132.

———; M. MASUTANI, A. LEETMAA, H. RUI, M. JI and A. KUMAR. 1997. Teleconnective response of the Pacific-North American region atmosphere to large central equatorial Pacific SST anomalies. *J. Clim.* **10**: 1787–1820.

MAGNUSON, J.J.; K.E. WEBSTER, R.A. ASSEL, C.J. BOWSER, P.J. DILLON, J.G. EATON, H.E. EVANS, E.J.

FEE, R.I. HALL, L.R. MORTSCH, D.W. SCHINDLER and F.H. QUINN. 1997. Potential effects of climate changes on aquatic systems: Laurentian Great Lakes and Precambrian shield region. *Hydrol. Proc.* **11**: 825–871.

MO, R.; J. FYFE and J. DEROME. 1998. Phase-locked and asymmetric correlations of the wintertime atmospheric patterns with the ENSO. ATMOSPHERE-OCEAN, **36**: 213–239.

MOLTENI, F. and S. TIBALDI. 1990. Regimes in the wintertime circulation over northern extratropics. II: Consequences for dynamical predictability. *Q.J.R. Meteorol. Soc.* **116**: 1263–1288.

MONTROY, D.L.; M.B. RICHMAN and P.J. LAMB. 1998. Observed nonlinearities of monthly teleconnections between tropical Pacific sea surface temperature anomalies and central and eastern North American precipitation. *J. Clim.* **11**: 1812-1835.

MYSAK, L.A.; R.G. INGRAM, J. WANG and A. VAN DER BAAREN. 1996. The anomalous sea-ice extent in Hudson Bay, Baffin Bay and the Labrador Sea during three simultaneous NAO and ENSO episodes. ATMOSPHERE-OCEAN, **34**: 313–343.

NAMIAS, J. 1978. Persistence of U.S. seasonal temperatures up to one year. *Mon. Weather Rev.* **106**: 1557–1567.

———. 1986. Persistence of flow patterns over North America and adjacent ocean sectors. *Mon. Weather Rev.* **114**: 1368–1383.

QUINN, F.H.; R.A. ASSEL, D.E., BOYCE, G.A., LESHKEVICH, C.R., SNIDER and D. WEISNET. 1978. Summary of Great Lakes weather and ice conditions, winter 1976–77. NOAA TM ERL GLERL-20, Great Lakes Environmental Research Lab., Ann Arbor, MI., 141 pp.

RENSHAW, A.C.; D.P. ROWELL and C.K. FOLLAND. 1998. Wintertime low-frequency weather variability in the North Pacific-American sector 1949–93. *J. Clim.* **11**: 1073-1093.

RODIONOV, S.N. 1994. *Global and Regional Climate Interaction: The Caspian Sea Experience.* Kluwer Academic. Pub., Dordrecht, The Netherlands, 241 pp.

——— and R.A. ASSEL. 1999. Laurentian Great Lakes ice cover and atmospheric teleconnection patterns: A decision-tree analysis. *In*: Proc. Eight Conference on Climate Variations, 13–17 Sept., Denver, CO, AMS, Boston, MA, pp. 38–43.

ROGERS, J.C. 1984. The association between the North Atlantic Oscillation and the Southern Oscillation in the Northern Hemisphere. *Mon. Weather Rev.* **112**: 1999–2015.

——— and H. VAN LOON. 1979. The seesaw in winter temperatures between Greenland and Northern Europe. Part II: Some oceanic and atmospheric effects in middle and high latitudes. *Mon. Weather Rev.* **107**: 509–519.

SERREZE, M.C.; M.P. CLARK, D.L. MCGINNIS and D.A. ROBINSON. 1998. Characteristics of snowfall over the eastern half of the United States and relationships with principal modes of low-frequency atmospheric variability. *J. Clim.* **11**: 234–250.

SHABBAR, A. and M. KHANDEKAR. 1996. The impact of El Niño-Southern Oscillation on the temperature field over Canada. ATMOSPHERE-OCEAN, **34**: 401–416.

The AnswerTree™ 2.0, User's Guide. 1998. SPSS Inc., Chicago, IL. 209 pp.

VAN LOON, H. and J.C. ROGERS. 1978. The seesaw in winter temperatures between Greenland and Northern Europe. Part I: General Description. *Mon. Weather Rev.* **106**: 296–310.

WALLACE, J.M. and D.S. GUTZLER. 1981. Teleconnections in the geopotential height field during, the Northern Hemisphere winter. *Mon. Weather Rev.* **109**: 784–812.

——— and Q. JIANG. 1992. On the observed structure of the interannual variability of the atmosphere/ocean climate system. In: *Atmospheric and Oceanic Variability*, H. Cattle (Ed.) Bracknell, U.K., pp. 17–43.

———; C. SMITH and Q. JIANG. 1990. Spatial patterns of atmosphere-ocean interaction in the northern winter. *J. Clim.* **3**: 990–998.

———; ——— and C.S. BRETHERTON. 1992. Singular value decomposition of wintertime sea surface temperature and 500-mb height anomalies. *J. Clim.* **5**: 561–576.

———; Y. ZHANG and K.H. LAU. 1993. Structure and seasonality of interannual and interdecadal variability of the geopotential height and temperature fields in the Northern Hemisphere Troposphere. *J. Clim.* **6**: 2063–2082.

WOLTER, K. and M.S. TIMLIN. 1998. Measuring the strength of ENSO – how does 1997/98 rank? *Weather*, **53**: 315–324.

YARNAL, B.M. and H.F. DIAZ. 1986. Relationships between extremes of the Southern Oscillation and the winter climate of the Anglo-American Pacific coast. *J. Climatol.* **6**: 197–219.

——— and D.J. LEATHERS. 1988. Relationships between interdecadal and interannual climatic variations and their effect on Pennsylvania climate. *Ann. Assoc. Am. Geogr.* **78**: 624–641.

ZHANG, Y.; J.M. WALLACE and N. IWASAKA. 1996. Is climate variability over the North Pacific a linear response to ENSO? *J. Clim.* **9**: 1468–1478.

ZORITA, E.; J.P. HUGHES, D.P. LETTEMAIER and H. VON STORCH. 1995. Stochastic characterization of regional circulation patterns for climate model diagnosis and estimation of local precipitation. *J. Clim.* **8**: 1023–1042.